

FULL SCALE MEASUREMENTS OF VELOCITY, REYNOLDS STRESS, SPECTRA AND COSPECTRA UPWIND AND AT THE CREST OF A LARGE HILL IN COMPLEX TERRAIN

D.C. STEVENSON AND D. NEAL

DEPARTMENT OF MECHANICAL ENGINEERING

UNIVERSITY OF CANTERBURY, CHRISTCHURCH, NEW ZEALAND

SUMMARY The velocity, turbulence, Reynolds stress, spectra and cospectra were measured in neutrally stable conditions on flat open terrain and compared with their values as the flow traversed the crest of a saddle in Gebbies Pass, New Zealand. For the flat terrain the measured values are generally in good agreement with other workers. At the crest the increase in turbulence was less than expected and reasons for this are discussed. The speed-up factor is compared with the theory of Jackson and Hunt and spectra are compared with Kaimal's model spectra. It was found that with suitable modifications, Kaimal's model spectra for flat homogeneous terrain fit the spectra and cospectra at the crest.

1 INTRODUCTION

The results in this paper are part of a study to measure the detailed wind structure over rural and complex terrain. The site used is a saddle in Banks Peninsula near Christchurch. Previous publications (Neal et. al. 1981, Neal 1982), have presented results for velocity profiles and comparisons between full scale measurements and wind tunnel tests. Some data has been presented on turbulence intensity and energy spectra. This paper briefly describes changes that occur to velocity profiles, turbulence and Reynolds stresses as the wind travels from flat terrain to the crest of a saddle 300 m high. Changes that occur to spectra and cospectra as the wind travels from flat terrain to the saddle are also given. Few researchers have produced information for complex terrain conditions. The most significant study in this regard is probably that of Bradley (1980) in his study of the profiles of wind speed, shearing stress and turbulence at the crest of Black Mountain in Canberra, Australia. Unfortunately, he did not measure spectra or cospectra at both the upwind and crest sites to permit comparison with those measured in this study.

2 DESCRIPTION OF TERRAIN

The Gebbies Pass region on Banks Peninsula has been described fully by Neal et. al. (1981). A schematic diagram of the major terrain features is given in Figure 1. This view is taken from the NE of the region and looks SW.

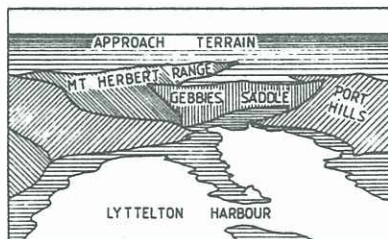


Figure 1 Terrain features of the Gebbies Pass region. (Heights: Port Hills 600 m; Gebbies Saddle 300 m; Mt Herbert Range 500 m).

A sketch of the crest section through the saddle is given in Figure 2 and the value of the saddle slope $H/L \approx 0.5$.

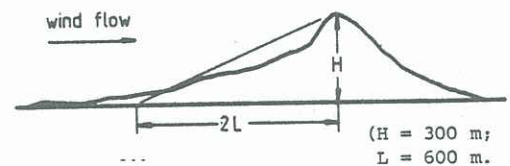


Figure 2 Approximate Gebbies Pass Saddle Cross Section

In the study by Bradley, the slope $H/L = 0.6$ and due to the physical similarities, his measurements are considered particularly relevant to the Gebbies Pass study. The approach flow is measured at a point on the windward side of the saddle and is referred to as Field Point 1. The second point is at the crest of the saddle denoted as Field Point 15. The Gebbies Pass region is a farming area and is covered with short grass which is grazed although some cropping is carried out. Shelterbelts 10-12 m high and scrub areas 2-6 m high exist on both the approach terrain and Gebbies Saddle. This type of terrain corresponds to roughness generally denoted as farmland in ESDU (1974) classification of terrain types and should have a roughness length of between .02 and .1 m. SW wind flows common in this region are cold, strong and often associated with heavy cloud cover. When measurements were carried out there was virtually no convection and neutral stability conditions were assumed.

3 EQUIPMENT

Measurements at Field Point 1 were made using 4 arrays of 3 Gill-type propeller anemometers mounted orthogonally at 5.3, 10.3, 15.3 and 19.2 m and spaced vertically up a 20 m tower. At Field Point 15 the 20 m tower was instrumented at 3 heights, namely 10.3, 15.3 and 19.2 m. At Field Point 1 a second series of tests was carried out using 4 Rimco fast response cup anemometers mounted from 1-4 m high in order to verify the value of Z_0 . Simultaneous measurements from the 3 anemometers at each point enabled the instantaneous wind vector to be determined as a function of time. The anemometers are four-bladed 190 mm diameter polystyrene propellers. Each propeller drives a shaft-mounted disc containing 32 slots. The disc rotates between two pairs of light emitting diodes and photo-receivers. Each of the photo-receivers produces a square wave and the relative positions of the two square waves are such that they are 90° out of phase. From this the direction rotation is determined. The square waves with a frequency 32 times the rotational speed of the propeller drive an 8-bit counter which integrates the counts over a selected period. The counts indicating velocity and

direction are written on a 7-track digital magnetic tape. Suitable programs were written in Algol to enable detailed analysis on the University Burroughs 6718 computer.

Normal precautions were taken to prevent aliasing errors due to sampling rate and linear or parabolic trends were removed from the data. The program analysing the data included a correction procedure for any possible non-vertical alignment of the vertical component anemometers. A cosine directional correction was applied to the propeller but no correction was made for anemometer frequency response. The length of run analysed for each measurement was 72 or 37 minutes depending on the prevailing weather conditions.

4.1 Velocity Profiles

Figure 3 shows the velocity profiles measured at Field Points 1 and 15. The GP symbols refer to different wind events with the mean velocity varying from 10 to 15 m/s at 10.3 m. Wind tunnel model profiles are also shown. Tala kite data to a height of 240 m was also obtained at both field points and a correlation always greater than 0.85 was obtained between different wind events. The Tala kite data verified and extended the tower data and at the crest of the almost uniform velocity profile, continued to at least 240 m. There is evidence of a "jet" or maximum velocity at the crest at a height of 15 m. Bradley noticed a similar phenomenon but at a height of 30 m for his conditions. There was no evidence of a jet in the wind tunnel model profiles.

Velocity profiles for the approach terrain measured by both the propellers and the Rimco anemometers gave a roughness length Z_0 of 0.025 m in good agreement with ESDU (1974) for this type of terrain. The power law exponent α was 0.16 which is consistent with flat rural terrain. Using a value of 0.4 for von Karman's constant and the slope of the velocity-height graph, the value of u_* was determined at Field Point 1 in addition to the value calculated from \overline{uw} . At Field Point 15 because of the almost vertical velocity profile, only \overline{uw} could be used to obtain u_* . It was found that the friction velocity increased by a factor of 1.6 at the crest of the saddle.

The average speed-up ratio $\Delta S = \Delta u/u_1$ was 0.6. This is less than the theoretical value of Jackson and Hunt of 1.0 given by $\Delta S \approx 2h/L$. In this case, the ratio of $h/L = 0.5$ is very much higher than the assumptions allow in the theory of Jackson and Hunt.

4.2 Turbulence Profiles

4.2.1 Longitudinal Component σ_u

On the flat approach terrain σ_u/u_* was measured as 2.17 \pm 0.04 and appeared to be invariant with height up to 19.2 m. The value is in good agreement with Bradley (1980) who obtained a value of 2.2.

At the crest σ_u/u_* increased by a factor of 1.1 with little variation with height (Figure 4a). This is much

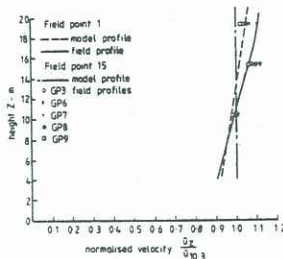


Figure 3 Velocity profiles at Field Points 1 and 15

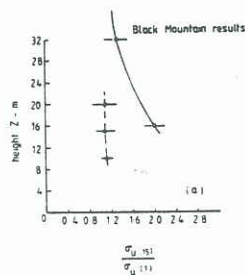


Figure 4 Variation of σ_u and σ_w between Field Points 1 and 15

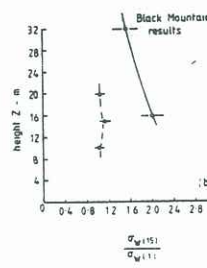
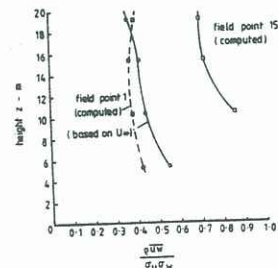


Figure 5 \overline{uw} Reynolds stress profiles for Field Points 1 and 15



less than Bradley which showed a doubling at lower heights ($z - d = 9$ m) but only a slight increase at 87 m height. Although the mast height is relatively small compared with the hill height, it is possible that the inner layer is quite small. Figure 2 shows there is a sudden steepening of the slope near the crest and this "hill on a hill" effect would reduce the inner layer thickness. Correcting for the displacement thickness d in Bradley's data would reduce disagreement slightly. The results for \overline{uw} shown in Figure 4b showed a similar behaviour. The value of \overline{uw}/u_* in the approach flow was 1.10 ± 0.15 with little increase as the wind traversed the crest and not much variation with height. Bradley records a value of 1.20 ± 0.13 in the approach flow but at the crest this doubles at lower heights (9 m) and is about 1.6 times as much at 87 m.

The possibility of low pass filtering at lower heights for the vertical anemometer in particular is discussed later.

4.3 Reynolds Stress \overline{uw}

Figure 5 shows the Reynolds stress for Field Point 1, which was obtained for the approach flow by two methods: 1) calculated from the propeller anemometers; 2) determined from the friction velocity u_* by the expression $u_*^2 = \overline{uw}$

At Field Point 1 the differences between the two methods are less than 10% except for the lowest array of anemometers at 5.3 m. If there was an effect of low pass filtering due to the lack of response of the vertical propellers, then the value of \overline{uw} would be underestimated. This would increase near the surface as the frequency of turbulence increased. The value of \overline{uw} would also be affected, tending to cancel out the total effect on $\overline{uw}/\sigma_u \sigma_w$. However, the value of Reynolds stress calculated from the friction velocity and normalised by σ_u and σ_w would be too high as shown in Figure 5, due to the underestimation of σ_w .

On the approach terrain the normalised value for the Reynolds stresses of -0.4 is a little higher than Teunissen (1980) who obtained -0.31 and higher than ESDU (1974) which gives -0.27 for $Z_0 = 0.03$ m. They are slightly higher than Flay et. al. (1982) who give -0.36 for similar terrain.

At Field Point 15 the Reynolds stress is also shown in Figure 5 and appears to be more dependent on height. At 10.3 m it is increased by a factor of 2.5 which is in good agreement with Bradley (1980) at a height of 20 m. Below 20 m Bradley found that the Reynolds stress increased but found a maximum at 30 m in the region of low shear at the "jet". This minimum was not clearly apparent in the present tests, possibly because of too few points measured.

4.4 Spectra

Kaimal et. al. (1982) proposed spectra for the three components of turbulence for flat homogeneous terrain. These model spectra used the friction velocity as a

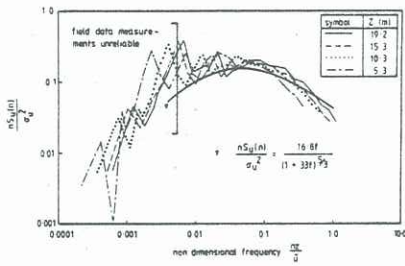


Figure 6 Longitudinal component of the energy spectrum for Field Point 1

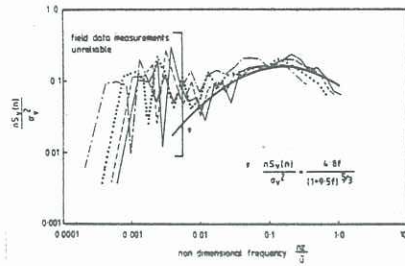


Figure 7 Lateral component of the energy spectrum for Field Point 1

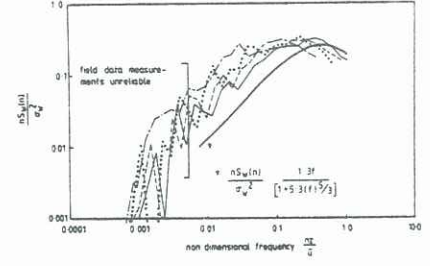


Figure 8 Vertical component of the energy spectrum for Field Point 1

normalising factor. To make Kaimal's spectra comparable with the present ones using the variance as the normalising factor, the following relationships were used:

$$\sigma_u = 2.5 u_* \quad \sigma_v = 1.875 u_* \quad \sigma_w = 1.25 u_*$$

4.4.1 Spectra on Approach Terrain

Figures 6, 7 and 8 show the spectra for the u , v and w components and the modified Kaimal expressions are both shown and plotted. Agreement is good for the u and v components down to the lower limit of reliability of the field data. The low frequency component of the w component is much larger than the Kaimal expression. It is possible that the normalising factor σ_w is too small thus making the spectra appear to be too high. Because the w spectra are of higher frequency than the u spectra a fall-off at the higher frequencies is likely because of the reduction in high frequency response of the propeller anemometer.

For the u and v spectra the position of the peak is in good agreement with Kaimal's model spectra. There is always the possibility that even a slight amount of convection would increase the low frequency spectra particularly in the case of the u component. There is some indication of this in Figure 6 but it is not great so the assumption of neutral stability is reasonable. Nonetheless, it would have been valuable to have temperature measurements to confirm this.

Teunissen (1980) did measure temperature gradients and confirmed near-neutral stability of his boundary layer. However, he did find the spectral density at lower frequencies of all turbulence components to be high and proposed "terrain scaling" parameters. Teunissen suggested that generally rougher gross features in the upstream terrain may have been responsible; a similar situation to the present tests.

4.4.2 Spectra at Crest of Saddle

Figures 9, 10 and 11 give the ranges of spectra for u , v and w at Field Point 15 over a period of a year. A modified Kaimal expression is shown and plotted on these

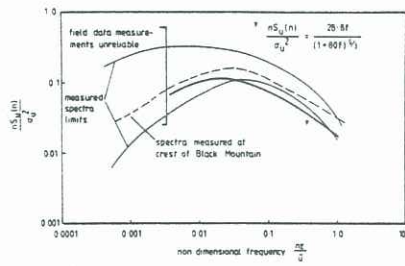


Figure 9 Range of measured longitudinal component of the energy spectrum for Field Point 15

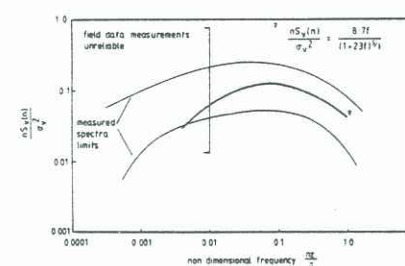


Figure 10 Range of measured lateral component of the energy spectrum for Field Point 15

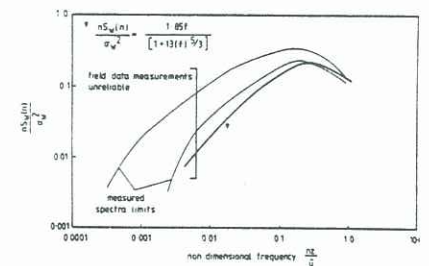


Figure 11 Range of measured vertical component of the energy spectrum for Field Point 15

Figures as well as u spectra in Figure 8 for the crest of Bradley's (1980) Black Mountain results.

The model spectra proposed by Kaimal are based on flat homogeneous terrain and are normalised by the friction velocity u_* . There is an increase in u_* from Field Point 1 to Field Point 15 and the effect of this change could be accounted for by the introduction of a term $\beta = (u_{*crest}/u_{*flat})^2$. The modified model spectra are quoted and plotted in Figures 9, 10 and 11.

The peaks of all the velocity components are moved to lower frequencies and increased in magnitude. The peaks of the modified Kaimal expressions agree well with the actual measured peaks but the low frequency spectral density for the measured v and w components are greater than the modified Kaimal expressions. The underestimation of σ_w has been discussed earlier but the possibility of some convection affecting all the components cannot be ruled out.

4.5 Cospetra

The cospetra for Field Points 1 and 15 are shown in Figures 12 and 13 and are compared with Kaimal's unmodified model spectra. The magnitudes shape and peak positions are in good agreement for Field Point 1.

The spread of measured results at higher frequencies is eliminated if the data is plotted against frequency. This is particularly noticeable for the flat terrain but also applies to the crest where the nearly uniform velocity profile hides the invariant behaviour of the cospetra with height. This agrees with the theory that in the inertial subrange the cospetral intensity is a function of f .

At the crest the spectral intensity is less than Kaimal's formula. The formula proposed on Figure 12 is obtained by reducing Kaimal's model formula by a factor $\sqrt{\beta}$ or the inverse ratio of the friction velocities. The agreement is then very good but the use of $\sqrt{\beta}$ may be fortuitous.

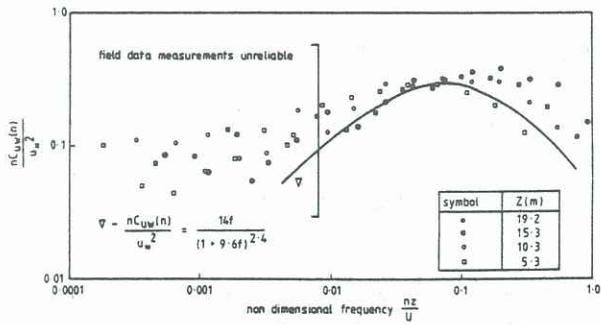


Figure 12 Cospectra measured at Field Point 1

5 CONCLUSIONS

1. The measured values of roughness length, velocity profile, turbulence and Reynolds stress are in reasonable agreement with other workers for similar flat terrain.
2. The spectra for flat terrain for the vertical velocity component is too high at low frequencies probably because of underestimation of the vertical variance due to a fall-off in high frequency response of the propeller anemometer.
3. On the flat, cospectra showed good agreement with Kaimal if plotted against frequency.
4. At the crest there is an almost uniform velocity profile but the variance of both u and w do not increase as much as expected. Low pass filtering particularly for the vertical propeller, is probably the reason.
5. The Reynolds stress at the crest is more than doubled in fair agreement with Bradley.
6. The spectra at the crest agree with Kaimal's model formula if they are modified by a factor β equal to the square of the ratio of the friction velocities at the crest and on the flat. The effect of low pass filtering by the vertical anemometer is still apparent.
7. The cospectra at the crest agree with a modified Kaimal expression reduced by a factor of $\sqrt{\beta}$.

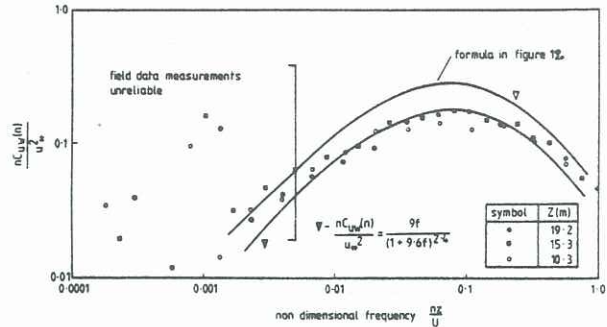


Figure 13 Cospectra measured at Field Point 15

6 REFERENCES

- BRADLEY, E.F. (1980) An experimental study of the profiles of wind speed, shearing stress and turbulence at the crest of a large hill. *Quart. J.R. Met. Soc.*, **106**, 101-123.
- FLAY, R.G.J., STEVENSON, D.C. and LINDLEY, D. (1982) Wind structure in a rural atmospheric boundary layer near the ground. *J. of Wind Eng and Ind. Aero.*, **10**, 63-78.
- JACKSON, P.S. and HUNT J.C.R. (1975) Turbulent wind over a low hill. *Quart. J.R. Met. Soc.* **101**, 929-955.
- KAIMAL, J.C., WYNGAARD, J.C., IZUMI, Y. and COTE, O.R. (1972) Spectral characteristics of surface-layer turbulence. *Quart. J. R. Met. Soc.*, **98**, 563-589.
- NEAL, C., STEVENSON, D.C., and LINDLEY, D. (1981) A wind tunnel boundary-layer simulation of wind flow over complex terrain: Effect of terrain and model construction. *Boundary Layer Meteorology*, **21**, 271-293.
- NEAL, D. (1982) Full scale measurements of the wind regime over a saddle and correlation with wind tunnel tests. *Boundary Layer Meteorology*, **22**, 351-371.
- TEUNISSEN, H.W. (1980) Structure of mean winds and turbulence in the planetary boundary layer over rural terrain. *Boundary Layer Meteorology*, **19**, 187-221.